FEMS Microbiology Ecology, 96, 2020, fiaa034

doi: 10.1093/femsec/fiaa034
Advance Access Publication Date: 4 March 2020
Research Article

RESEARCH ARTICLE

Shifts in short-chain fatty acid profile, Fe(III) reduction and bacterial community with biochar amendment in rice paddy soil

Yue Lu[1,2,*], Leiling Fu[1,2], Lin Tang[1,2,*], Jing Zhang[3], Yanru Zhang[1,2], Jingjing Wang[1,2], Qingqing Xie[1,2], Zhaohui Yang[1,2], Changzheng Fan[1,2] and Shoujuan Zhang[1,2]

[1]College of Environmental Science and Engineering, Hunan University, Changsha, 410082, Hunan, China, [2]Key Laboratory of Environmental Biology and Pollution Control (Hunan University), Ministry of Education, Changsha, 410082, Hunan, China and [3]School of Agriculture and Biology, Shanghai Jiao Tong University, Shanghai 200240, China

*Corresponding author: College of Environmental Science and Engineering, Hunan University, South Lushan Road, Changsha, 410082, PR China. Tel: +86-13107228851; Fax: +86-731-88822829; E-mail: yuelu@hnu.edu.cn and tanglin@hnu.edu.cn

One sentence summary: Amendment of different types of biochar altered SCFA profile, Fe(III) reduction and bacterial biodiversity in rice paddy soil.

Editor: Angela Sessitsch

ABSTRACT

Biochar, a valuable product from the pyrolysis of agricultural and forestry residues, has been widely applied as soil amendment. However, the effect of different types of biochar on soil microorganisms and associated biochemical processes in paddy soil remains ambiguous. In this study, we investigated the impact of biochars derived from different feedstocks (rice straw, orange peel and bamboo powder) on the dynamics of short-chain fatty acids (SCFAs), iron concentration and bacterial community in paddy soil within 90 days of anaerobic incubation. Results showed that biochar amendment overall inhibited the accumulation of SCFAs while accelerating the Fe(III) reduction process in paddy soil. In addition, 16S rRNA gene sequencing results demonstrated that the α-diversity of the bacterial community significantly decreased in response to biochar amendments at day 1 but was relatively unaffected at the end of incubation, and incubation time was the major driver for the succession of the bacterial community. Furthermore, significant correlations between parameters (e.g. SCFAs and iron concentration) and bacterial taxa (e.g. *Clostridia*, *Syntrophus*, *Syntrophobacter* and *Desulfatiglans*) were observed. Overall, our findings demonstrated amendment with different types of biochar altered SCFA profile, Fe(III) reduction and bacterial biodiversity in rice paddy soil.

Keywords: biochar; short-chain fatty acids; Fe(III) reduction; high-throughput sequencing; bacterial community; paddy soil

INTRODUCTION

Sustainable development emphasizes the conversion of waste into renewable energy, and of the waste sources, the low toxicity and large quantity of biomass residues has stirred extensive research interest worldwide (Qambrani *et al.* 2017; Ramos *et al.* 2018). In China, ~174–249 million tons of crop residues and ~1081 million tons of forestry waste are produced each year (Chen 2016; Xie *et al.* 2018), which provides a considerable amounts of biomass feedstock. Biochar, a porous and carbon-rich solid intentionally derived from biomass and green waste

Received: 6 December 2019; **Accepted:** 3 March 2020

by a pyrolysis process, has been proposed for large-scale applications, such as adsorbing pollutants in wastewater, contaminated soils and sediments (Wang *et al.* 2017a; Qiao, Li and Li 2018; Tang *et al.* 2018; Wang *et al.* 2019a), increasing crop yields in nutrient-poor soils by holding nutrients and building fertility (Hussain *et al.* 2016), as well as improving soil quality and mitigating global climate change through carbon sequestration (Abdel-Fattah *et al.* 2015; Agegnehu, Srivastava and Bird 2017). Hence, the addition of biochar to the environment enables the reuse of waste and may have beneficial effects on the ecosystem.

Previous studies have demonstrated that biochar addition had a positive effect on pH (Liu *et al.* 2016), total carbon content (Lu *et al.* 2014) and available phosphorus (Gul and Whalen 2016), while having a negative effect on CH_4 emission (Wang *et al.* 2019b) and N_2O emission (Cayuela *et al.* 2014) in soil. Fe(III) reduction is an important biochemical process in paddy soil, and biochar was found to accelerate Fe(III) reduction due to its ability to increase the production of dissolved organic carbon (Jia *et al.* 2018) and to stimulate the activity of fermentative Fe(III)-reducing microorganisms (Tong *et al.* 2014; Wang *et al.* 2017b). In addition, short chain fatty acids (SCFAs) such as acetate, propionate and formate, the main metabolic products of anaerobic bacteria fermentation in paddy fields, could serve as electron donors for those iron-reducers and other functional microbes (He and Qu 2008), and biochar amendment might also lead to a shift in the accumulation/consumption of SCFAs in paddy soil. In an anaerobic digestion system, the addition of biochar was found to reduce the maximum accumulation of fatty acids during anaerobic composting of sludge, which was mainly due to an increase in the SCFA-utilizing bacterial population (Awasthi *et al.* 2018). Biochar as an electron transfer mediator could also promote the syntrophic oxidation of SCFAs in the anaerobic digestion process, and with the accumulation of fatty acids, the pH buffering capacity introduced by biochar was observed to maintain stable pH and efficient methane production (Wang *et al.* 2018). However, our knowledge of the effect of biochar amendment on the shift of SCFAs and iron profile in paddy soil is rather limited.

Adding biochar also alters the bacterial abundance and community structure in rice paddy soil. For instance, a 6-week study showed that biochar amendment substantially changed the α-diversity of the bacterial population and significantly increased the relative abundance of *Flammeovirgaceae* and *Chitinophagaceae*, which both have an important role in organic matter decomposition (Yoon *et al.* 2007), and *Hyphomicrobiaceae*, which are able to modulate and fix nitrogen (Xu *et al.* 2014a), while in a 5-month anaerobic incubation experiment and a 6-year field experiment, biochar addition did not lead to a significant change of bacterial abundance and community structure (Tian *et al.* 2016; Song *et al.* 2017). Considering that the composition of biochar largely depends on the feedstocks, the amendment of different types of biochar to soil may result in diverse impacts on the bacterial community. A recent study showed that adding biochar derived from rice straw, manure or wood chips to rice paddy soil resulted in different changes of dominant bacterial taxa, e.g. *Proteobacteria*, *Actinobacteria*, *Chlorobi* and *Bacteroidetes*. In addition, a significant enrichment of *Clostridium* and *Thermincola* was found in manure biochar and wood chip biochar amended soil, respectively (Yuan *et al.* 2018). Biochar generated from different sources of feedstock shows variance in functional groups, surface area and carbon content, which might explain the dissimilar response of the bacterial community to biochar amendment in paddy soil (Kloss *et al.* 2012; Zhao *et al.* 2013).

Therefore, to investigate whether biochar addition would have an effect on SCFAs profile, Fe(III) reduction and bacterial biodiversity in paddy soil and whether different types of biochar would have different effects, three biochars derived from rice straw (RB), orange peel (OB) and bamboo powder (BB) were added to paddy soil respectively and incubated anaerobically in the laboratory for 90 days. Our objectives were: (i) to characterize the chemical composition and properties of the three biochars; (ii) to investigate the influence of biochar amendment on SCFAs and iron variation in rice paddy soil during the incubation; (iii) to determine the response of bacterial community structure and abundance to biochars and the correlation between bacterial taxa and environmental variables over incubation time.

MATERIAL AND METHODS

Biochar preparation and characterization

Rice straw, orange peel and bamboo powder, representing different feedstocks from forestry and agricultural residues, were collected and used for biochar production. Before the pyrolysis step, those feedstocks were dried at 60°C and pulverized into powder. Then, three types of biochar, i.e. RB, OB and BB were prepared in a furnace (SK-G04123K, China) at 600°C for 1 h with a constant flow of N_2 during the pyrolysis. The products were then vacuum filtered with 1 M HCl solution and ultrapure water several times to remove dust and dried at 60°C. Finally, three types of biochar were sieved (a 100-mesh sieve) separately and stored at room temperature until use.

Biochar was mixed with deionized water (1:10 ratio, v/v) for pH measurement with a pH probe (Leici Instrumentation Factory, PHS-3C, China). The morphology and elemental distribution were observed by a scanning electron microscope (SEM, Hitachi S4800, Japan), operating at 20 kV with an energy dispersive X-ray detector. X-ray photoelectron spectroscopy (XPS, Thermo Scientific, Escalab 250XI, USA) was used to determine the elemental composition, and the surface functional groups were studied by Fourier transform infrared spectroscopy (FTIR, Thermo Scientific, Nicolet 5700, USA).

Soil sampling and incubation

Soil from the plow layer (0–20 cm) was sampled from a rice paddy field in Xiangtan (27°53'N, 112°31'E), Hunan province, China in November 2018. Soils from six nearby sampling plots was fully mixed, air-dried and sieved with a mesh size of 2 mm.

For batch experiments, 10 g of paddy soil and 20 mL of N_2-flushed, ultra-pure water were added into serum bottles (120 mL), which afterwards were sealed with rubber stoppers and aluminum caps. The headspace was flushed with N_2 for 5 min to ensure an anaerobic atmosphere. For each biochar-amended treatment, 0.1 g of biochar (RB, OB or BB) was added separately, and bottles without biochar addition (NB) were set up as a control. Each treatment was prepared in triplicate and incubated at 30°C without shaking. On eight different sampling days (day 0, day 1, day 5, day 15, day 40, day 60, day 70 and day 90), 12 bottles (4 treatments × 3 replicates) were sacrificed for further analysis. The samples taken after 2 h of incubation were identified as day 0.

Chemical measurements

The pH value and water content of samples taken during the 90 days of incubation were measured as described before (Lu *et al.*

2015). The ferrous iron was extracted by 4.5 mL of 0.5 M HCl from 0.5 mL of soil suspension at 25°C for 24 h and the total iron was reduced to ferrous iron by hydroxylamine hydrochloride at 60°C for 2 h after extraction. Then the concentration of ferrous iron was determined using a 1,10-phenanthroline colorimetric assay after centrifugation at 5000 rpm for 5 min, and the ferric concentration was calculated as the difference in value between total iron and ferrous iron (Ma, Conrad and Lu 2012). To analyse SCFAs, e.g. acetate, propionate, butyrate, isobutyrate, valerate and isovalerate, 1 mL of filtrate from the soil suspension was collected through a 0.45 μm syringe fliter in a 1.5 mL gas chromatography vial, and 3% H_3PO_4 was added to adjust the pH to ~3.0. A gas chromatograph (Agilent Technologies, 7890A, USA) equipped with a flame ionization detector (FID), a thermal conductivity detector (TCD) and an Agilent DB-FFAP column (30 m × 0.32 mm × 0.5 mm) was utilized to determine the concentration of six SCFAs (Yuan *et al.* 2006).

High-throughput sequencing of bacterial 16S rRNA genes

At different time points of destructive sampling, fresh slurry from each bottle was collected and stored at −80°C. The samples taken at days 0, 1, 15, 40 and 90 during anaerobic incubation were selected for molecular analysis. Total genomic DNA in 0.5 g of the slurry samples was extracted by DNeasy PowerSoil Kit (Qiagen, Germany) according to the protocol described by the manufacturer. The quality and quantity of extracted DNA were measured using NanoDrop 2000 (Thermo Scientific, USA) and agarose gel electrophoresis (Tanon 2500, China). PCR amplification of the V3–V4 region of bacterial 16S rRNA genes was carried out on a My Cycler thermal cycler (Bio-Rad 580BR, USA) with the primer set: 343F (5′-TACGGRAGGCAGCAG-3′) and 798R (5′-AGGGTATCTAATCCT-3′). The amplicons after a quality test with gel electrophoresis were purified with Agencourt AMPure XP beads (Beckman Coulter, USA). After another round of amplification and purification, those amplicons were quantified using a Qubit dsDNA assay kit (Life Technologies Q32852, China). Finally, the purified PCR amplicons were equimolarly pooled and sequenced on an Illumina MiSeq platform at Shanghai OE Biotech. Co., Ltd. (Shanghai, China).

Raw sequencing data were preprocessed using Trimmomatic software (Bolger, Lohse and Usadel 2014) to detect and cut off ambiguous bases ('N' bases: representing bases that unsequenced and undefined) and low quality sequences. After trimming, paired-end reads were assembled using FLASH software (Reyon *et al.* 2012), and the sequence data were further quality-filtered to abandon reads with ambiguous, homologous sequences or those with length was <200 bp. Reads with 75% of bases above Q20 were retained. Then, reads with chimera were detected and removed by QIIME software (version 1.8.0) (Caporaso *et al.* 2010). After removing primer sequences, clean reads were clustered to generate operational taxonomic units (OTUs) using Vsearch software at the 97% similarity level (Edgar *et al.* 2011). The representative read of each OTU that was selected using the QIIME package was annotated and blasted against the SILVA database using the ribosomal database project (RDP) classifier with a confidence threshold of 70% (Wang *et al.* 2007).

Statistical analysis

OriginPro 8 was used to conduct the data processing and one-way analysis of variance (one-way ANOVA). α-Diversity including Chao1, Simpson and Shannon indices were calculated in the R package Vegan (Oksanen *et al.* 2008). Bray–Curtis distance was calculated from the OTUs abundance table as a measure of between-community (β) diversity. A heatmap based on Bray–Curtis distance and non-metric multidimensional scaling (NMDS) based on OTUs abundance were used to visualize the difference among samples and potential clustering by R software (Zuur, Ieno and Meesters 2009) and CANOCO 5.0 package (ter Braak and Smilauer 2012), respectively. Linear discriminant analysis (LDA) effect size (LEfSe) revealed the significantly different species in relative abundance among control and biochar-amended treatments. Spearman's correlation coefficients were calculated to determine the correlation between bacterial community and environmental variables and the heatmaps were created by R software.

Nucleotide sequences accession number

Nucleotide sequence data reported in this study were deposited to National Center for Biotechnology Information (NCBI) under bioproject number (PRJNA578799) and accession number (SRP226572).

RESULTS

Chemical and morphological properties of biochars

Three different feedstocks were applied to generate biochars, i.e. RB, OB and BB. Table 1 shows that biochars varied considerably in chemical properties including pH, C (%), N (%) and O (%) depending on the type of feedstock. It was noticed that the pH of OB (7.9) was lower than that of RB (8.3) and BB (8.6), which might be due to the different content of alkali metals (e.g. Mg and Ca) in the original feedstocks as previously reported (Abdelhafez and Li 2016). Elemental analysis showed that C and O were the dominant elements present in all three biochars, accounting for 88.86–94.27% and 5.73–9.49% of element composition, respectively. In addition, the morphological properties of biochars varied considerably depending on the feedstock type. SEM images showed RB with a smooth, elongated appearance with ordered porous structure (Fig. 1A), while a more smooth appearance was observed in BB with visible porous (Fig. 1C), and OB had a rough, irregular appearance and almost no visible porosity (Fig. 1B).

The chemical compositions and structure of the three types of biochar were further characterized. The wide-scan XPS spectra (Fig. 1D) show that the three biochars all have low O:C atomic ratios (0.06–0.11), and the C 1 s XPS spectra results reveal the same oxygen and carbon functional groups across the three types of biochar. Deconvolution of the C 1 s spectra of RB, BB and OB were fitted into three peaks, namely, aromatic C−C/C = C at 284.3–284.4 eV, C−O at 285.3–286.2 eV and O−C−O/C = O at 288.1–293.6 eV (Figs 1E–G). In all samples, the dominant functional groups were C−C/C = C, which was mainly contributed by the abundant carbon of biochars. These results were supported by FTIR spectra which could also indicate the surface functional groups in the biochars (Fig. 1H). The FTIR spectral properties of RB showed obvious absorption for the C = C, O−H and C = O stretching vibration at 1397 cm^{-1}, 1636 cm^{-1} and 3397 cm^{-1}, respectively. Also according to previous reports, the band at 1085 cm^{-1} reflected the vibration of C−O, and both of 796 cm^{-1} and 882 cm^{-1} bands could be assigned to C−H stretching vibrations (Xiao, Chen and Zhu 2014, Lu *et al.* 2017). Biochars OB and BB shared similar FTIR spectra, which showed weaker C−O and C = O absorption in comparison to RB, probably due to the higher oxygen content in RB.

Table 1. Chemical properties of three types of biochar.

Biochar	Feedstock	Pyrolysis temperature (°C)	pH	C (%)	N (%)	O (%)
RB	Rice straw	600 for 1 h	8.3	88.86	1.66	9.49
OB	Orange peel	600 for 1 h	7.9	93.61	0.5	6.39
BB	Bmboo powder	600 for 1 h	8.6	94.27	0.26	5.73

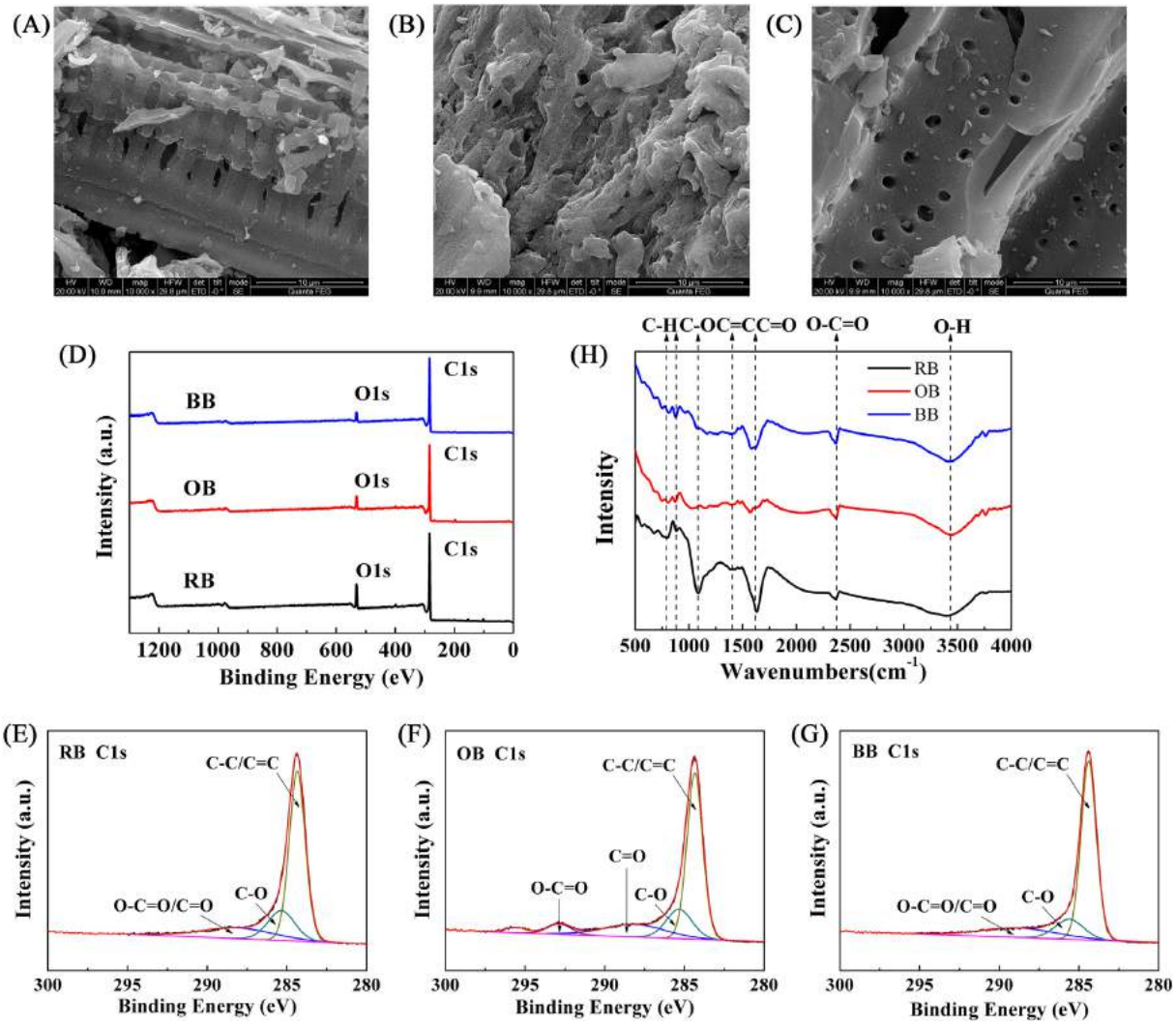

Figure 1. SEM images of (**A**) rice straw biochar (RB), (**B**) orange peel biochar (OB) and (**C**) bamboo powder biochar (BB); (**D**) XPS spectra of RB, OB and BB; C 1 s spectra of (**E**) RB, (**F**) OB and (**G**) BB; (**H**) FTIR spectra of the three types of biochar.

The variation in physicochemical properties of paddy soil after biochar amendment

The change of pH value (Fig. S1, see online supplementary material) followed a similar increasing trend with the four different treatments during incubation, leading ultimately to pH values ranging from 6.58 ± 0.03 (OB treatment) to 6.74 ± 0.02 (NB treatment) at day 90.

SCFAs including acetate, propionate, butyrate, isobutyrate, valerate and isovalerate were detected from the beginning of incubation (Fig. 2). With regard to overall acids, their concentrations undulated slightly within the first 15 days, and decreased sharply at day 40 to reach relatively low levels, and then increased slightly at the late stage (except for BB treatment at day 90). Specifically, acetate was the most abundant SCFA (up to 0.81 ± 0.04 mM) from day 1 and had a long presence time during the whole incubation, while propionate (up to 0.12 ± 0.02 mM), butyrate (up to 0.29 ± 0.02 mM) and valerate (up to 0.35 ± 0.02 mM) only accumulated in the early period and were completely consumed after day 40. During the 90 days of incubation, a low amount of isobutyrate (up to 0.07 ± 0.004 mM) was detected, and isovalerate (up to 0.19 ± 0.01 mM) was present except for on days 40 and 70. Biochar amendment (especially BB treatment) inhibited the accumulation of SCFAs on days 5, 60 and 90, and even acetate was depleted at day 90 with BB treatment.

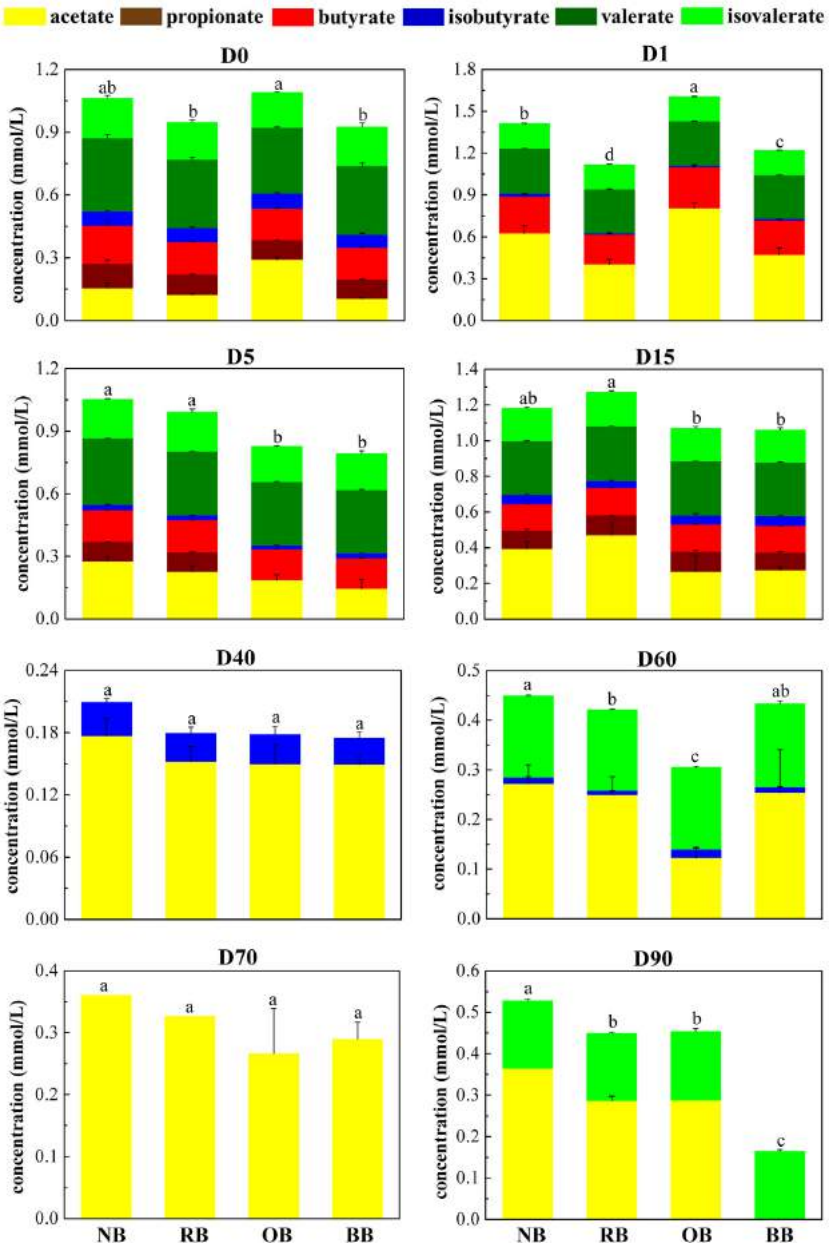

Figure 2. Effects of biochar addition on the production of SCFAs in paddy soil over incubation times. Error bars indicate standard deviation, $n = 3$. Different lowercase letters indicate significant differences between treatments on the same sampling day at the 5% level according to a one-way ANOVA test.

As shown in Fig. 3, the concentrations of Fe(II) in all treatments increased from the beginning and slightly decreased at the late stage. The change of Fe(III) showed different trends, which firstly increased at day 1 and declined afterwards but increased slightly at day 60. During the 90 days of incubation, biochar additions promoted the accumulation of Fe(II), especially for RB treatment at the late stage. For Fe(III) concentration, biochar additions had a positive effect on Fe(III) accumulation in the early stage (especially for BB at day 0 and OB at day 5), then an obvious transformation from Fe(III) to Fe(II) was observed from day 5 and, at the end of the incubation RB treatment had a higher concentration of Fe(III) than NB treatment.

Bacterial community diversity

A total of 2 086 060 valid tags were obtained through quality filtering from 60 soil samples (5 sampling dates × 4 treatments × 3 replicates), and the classified tags were clustered into 7932 OTUs with 97% sequence identity. The amount of OTUs in each sample ranged from 1456 to 3377 as shown in Table 2 and the OTU number in each sample had a sharp decrease at the early stage (day 1–15), then OTU number increased slowly and remained steady. Although OTUs of four treatments all recovered to a similar level at the end of incubation, the addition of biochar significantly increased the difference between the maximum and minimum number of OTUs, especially for the BB treatment.

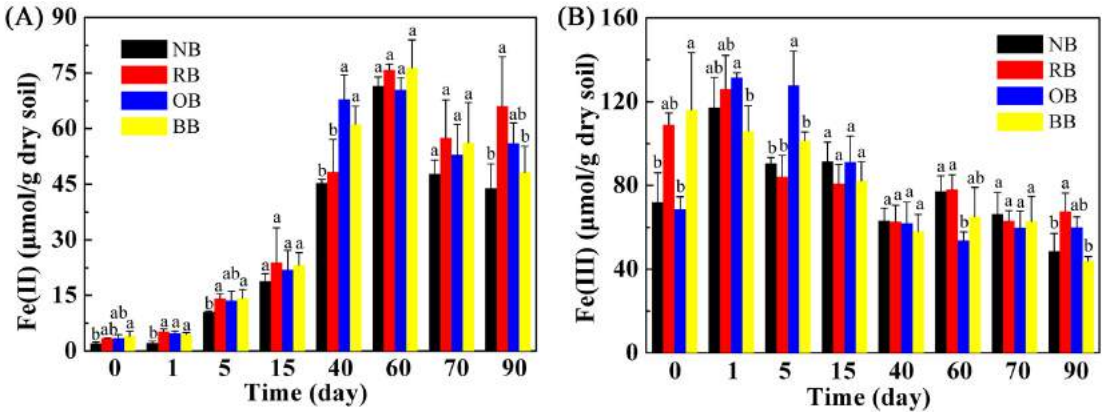

Figure 3. Effects of biochar amendment on (**A**) Fe(II) and (**B**) Fe(III) in paddy soil over incubation time. NB, RB, OB and BB represent non-biochar, rice straw biochar, orange peel biochar and bamboo powder biochar treatment, respectively. Error bars represent standard deviation, $n = 3$. Different lowercase letters indicate significant differences between treatments on the same sampling day at the 5% level according to a one-way ANOVA test.

Table 2. Bacterial community richness and diversity measured as OTU numbers, Chao1, Simpson and Shannon indices from different biochar treatments (NB, RB OB, and BB). Different lowercase letters indicate significant differences between treatments no the same sampling dye at the 5% level according to a one-way ANOVA test.

Time	Treatment	OTUs	Chao1	Simpson	Shannon
Day 0	NB	3295 ± 57 a	2741 ± 13 a	0.9941 ± 0.0003 ab	9.10 ± 0.07 ab
	RB	3219 ± 78 a	2727 ± 144 a	0.9941 ± 0.0006 ab	9.12 ± 0.10 ab
	OB	3237 ± 61 a	2806 ± 61 a	0.9939 ± 0.0001 ab	9.12 ± 0.07 ab
	BB	3387 ± 76 a	2785 ± 36 a	0.9947 ± 0.0004 ab	9.17 ± 0.09 a
Day 1	NB	2174 ± 64 cd	2125 ± 31 bc	0.9720 ± 0.0018 c	7.07 ± 0.06 d
	RB	1899 ± 60 d	1808 ± 37 d	0.9664 ± 0.0035 d	6.90 ± 0.06 de
	OB	2128 ± 126 cd	1982 ± 51 cd	0.9574 ± 0.0022 e	6.80 ± 0.09 e
	BB	2409 ± 84 bc	2048 ± 109 c	0.9684 ± 0.0029 cd	7.06 ± 0.15 d
Day 15	NB	2507 ± 46 bc	2248 ± 154 bc	0.9921 ± 0.0012 ab	8.63 ± 0.12 c
	RB	1980 ± 326 cd	2095 ± 19 bc	0.9917 ± 0.0013 ab	8.55 ± 0.12 c
	OB	1654 ± 85 de	2026 ± 126 cd	0.9911 ± 0.0012 b	8.58 ± 0.07 c
	BB	1483 ± 20 e	2105 ± 52 bc	0.9919 ± 0.0013 ab	8.62 ± 0.13 c
Day 40	NB	2324 ± 327 c	2230 ± 29 bc	0.9940 ± 0.0010 ab	8.86 ± 0.12 bc
	RB	2710 ± 50 b	2273 ± 94 b	0.9948 ± 0.0004 ab	8.91 ± 0.06 b
	OB	2691 ± 31 b	2162 ± 107 bc	0.9941 ± 0.0007 ab	8.84 ± 0.08 bc
	BB	2549 ± 69 bc	2144 ± 6 bc	0.9940 ± 0.0004 ab	8.82 ± 0.07 bc
Day 90	NB	2751 ± 61 b	2257 ± 45 bc	0.9951 ± 0.0003 a	9.00 ± 0.06 ab
	RB	2729 ± 73 b	2146 ± 89 bc	0.9950 ± 0.0002 ab	8.96 ± 0.05 ab
	OB	2480 ± 83 bc	2271 ± 51 bc	0.9948 ± 0.0002 ab	8.95 ± 0.06 ab
	BB	2523 ± 35 bc	2184 ± 71 bc	0.9948 ± 0.0002 ab	8.91 ± 0.06 b

Further OTU analysis (Fig. S2, see online supplementary material) showed that the number of core OTUs, total OTUs and their ratio had similar fluctuation during incubation, decreasing from day 0 to day 15, while increasing thereafter.

The α-diversity of the 16S rRNA gene-based bacterial community for four different treatments at five individual sampling days are shown in Table 2. The Chao1 index represents the richness of the microbial community, and Simpson and Shannon biodiversity indices are measures balancing between richness and evenness (Foggo, Rundle and Bilton 2003). The richness of the bacterial community initially was significantly higher than at the late stage, and then an obvious drop was observed in all treatments at day 1, especially with the RB treatment. Simpson and Shannon indices analysis showed a significant decrease of diversity in the bacterial community in the four different biochar treatments at day 1, the OB treatment in particular showed the most drastic loss. Noticeably, all treatments exhibited a recovery of evenness from day 15. Overall, the α-diversity of the bacterial community significantly decreased for a short time and reached a level equal to that in the initial paddy soil, and additions of biochar stimulated the decline of bacterial diversity especially at the early stage (day 1, especially for RB and OB treatment), which also slightly inhibited the recovery of α-diversity in paddy soil.

To further explore the succession of bacterial community during incubation and the effect of biochar amendments, NMDS were performed based on high-throughput sequencing data of 16S rRNA genes. As shown in Fig. 4, 60 samples were grouped into five envelopes by incubation time, and the differences were obviously narrowed with the process of incubation. However, the difference between the four different biochar treatments (NB,

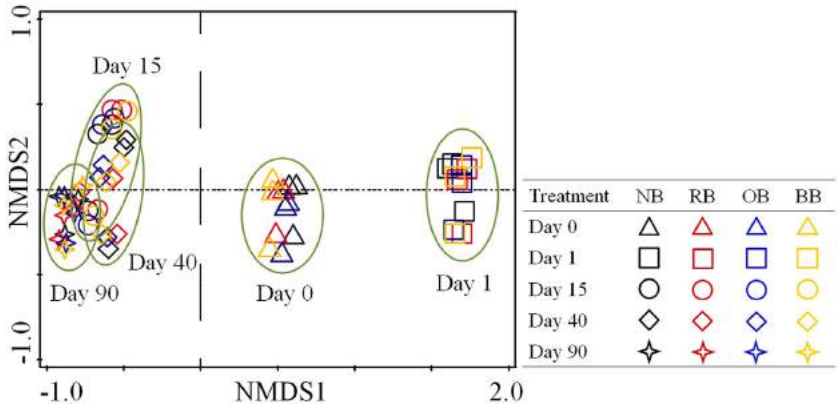

Figure 4. Non-metric multidimensional scaling (NMDS) shows the difference among samples based on bacterial composition. Different symbols indicate different sampling dates. Black, red, blue and yellow denote NB, RB, OB and BB treatments, respectively.

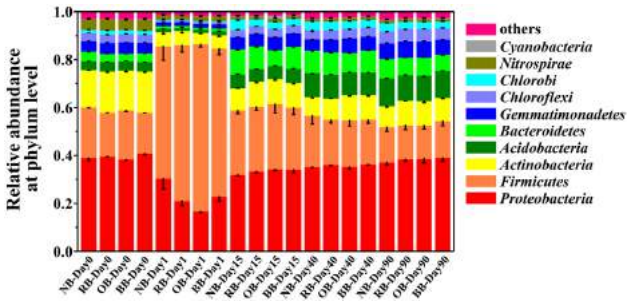

Figure 5. Succession of bacterial community in paddy soil amended with different types of biochar over incubation time at the phylum level (phyla with <1% relative abundance are grouped as 'others'). Error bars indicate standard deviation, $n = 3$.

RB, OB and BB) was rather indiscernible. Therefore, a more significant influence of incubation time on the bacterial community structure was identified in comparison to biochar amendment. Heatmap analysis based on Bray–Curtis distance was also applied to further statistically assess the succession of the bacterial community (Fig. S3, see online supplementary material). Bray–Curtis distance digitized the similarity of the two samples, and the heatmap visualized the distance by color (blue color represents higher similarity and red color lower similarity). The clustering and heatmap analyses were in good agreement with NMDS results, suggesting that the samples were clustered with incubation time and the effect of the biochar types was less obvious. Bacterial community at the late stage of incubation (especially days 40 and 90) showed high similarity, while samples at day 1 were separated and exhibited different bacterial composition, indicating a clear succession of the bacterial community with anaerobic incubation of paddy soil with/without biochar amendment. Permutational multivariate analysis of variance (PERMANOVA) further confirmed that incubation time was the major driver of the change in soil bacterial community composition rather than biochar addition (Table S1, see online supplementary material).

Bacterial community composition

The taxonomic composition in each sample was determined at both the phylum (Fig. 5) and class (Fig. S4, see online supplementary material) level to further explore the dynamics of the bacterial taxa during incubation. As shown in Fig. 5, among the bacterial taxa with relative abundance >1%, *Proteobacteria* (15.78–42.43%) and *Firmicutes* (9.90–71.87%) were the most dominant bacterial phyla in all samples, consistent with the results of a previous study (Li *et al.* 2016). The abundance of these two phyla showed a wide range of variation because of the short and dramatic reversal at day 1, and then *Proteobacteria* returned to the initial level, whereas *Firmicutes* decreased continuously with 6.5, 4.0, 6.4 and 1.4% loss compared with the beginning (day 0) with NB, RB, OB and BB treatments, respectively. The addition of three different types of biochar (especially OB) was beneficial to the abundance of *Firmicutes* but not *Proteobacteria*. Other bacterial taxa, such as *Actinobacteria* (3.55–18.12%), *Acidobacteria* (1.01–12.12%), *Bacteroidetes* (0.81–11.08%), *Gemmatimonadetes* (1.20–7.34%), *Chloroflexi* (0.64–5.78%) and *Chlorobi* (0.29–5.54%), were all detected in the initial samples, but showed an obvious decrease at day 1, and then increased gradually at the late stage. The relative abundances of these phyla were all higher at day 90 in comparison to day 0, except for *Actinobacteria*. At the class level (Fig. S4), *Clostridia* (9.33–60.63%) and *Deltaproteobacteria* (4.20–18.30%) were major classes during the incubation. *Clostridia* and *Bacilli* that belong to phylum *Firmicutes* showed a significant increase while *Deltaproteobacteria* (4.20–18.30%), *Alphaproteobacteria* (3.21–12.77%), *Betaproteobacteria* (3.17–15.31%) and *Gammaproteobacteria* (2.46–10.80%) that belong to phylum *Proteobacteria* decreased at day 1, contributing to the distinct change at phylum level.

Further, LEfSe analysis (Fig. 6) was conducted to identify the bacterial taxa that significantly differed among treatments at each taxonomic level. Biomarkers at each level could be used as candidate indicators to distinguish the difference of bacterial community among four different treatments. Initial differences among samples at day 0 could be explained by soil heterogeneity, and as the incubation proceeded, shifts in differential taxa were observed. No clear correlation between phylum-level biomarkers and class-level biomarkers was observed, which suggested the variance between the four treatments at class-level might be covered up after grouping different taxa to reach a higher taxonomic level. Additionally, the number of abundant taxa (significantly enriched at genus level) in the four treatments was decreased for a short time but increased after day 15. NB treatment always had more biomarkers than the other three biochar-amended treatments, indicating that biochar addition resulted in less differential taxa and the fluctuations in relative abundance were time-affected, which was in coordination with

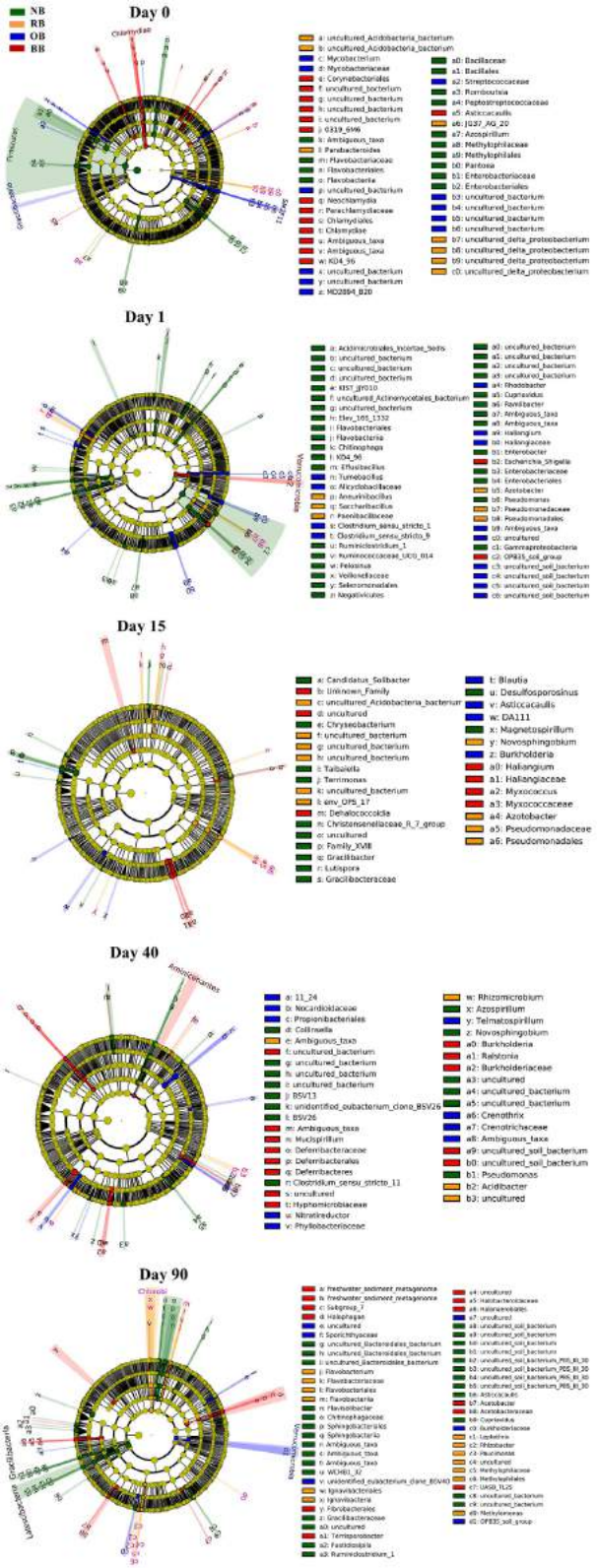

Figure 6. LEfSe analysis shows differences in relative abundance of the four groups at days 0, 1, 15, 40 and 90, respectively. The round dots with green, orange, blue and red color represent genera significantly enriched in NB, RB, OB and BB treatment, respectively ($P < 0.05$). Differing taxa are listed for each cladogram.

the decrease in OTU numbers and α-diversity at day 1 and the recovery after day 15.

The relationship between bacterial community and environmental variables

In order to reveal the response of bacterial community to environmental variables and experimental setting conditions including iron, six types of SCFA, three biochar types and incubation time, Spearman's correlation analysis were performed (Fig. 7). Results showed that diverse phyla were positively or negatively associated with incubation time, Fe(II), Fe(III) and SCFAs, while the effect of biochar amendment on the shift of bacterial community was less obvious. More specifically, at phylum level, the relative abundance of *Nitrospirae*, *Firmicutes* and *Deferribacteres* significantly decreased ($P < 0.05$) but *Acidobacteria*, *Bacteroidetes*, *Chlorobi* and *Chloroflexi* rose with the increase in pH value. In addition, phyla e.g. *Acidobacteria*, *Chloroflexi* and *Gemmatimonadetes* were positively correlated with Fe(II) and negatively associated with Fe(III). There were only a small number of phyla such as *Caldiserica*, *Chlamydiae*, *Firmicutes* and *Nitrospirae* that displayed positive correlation with almost all six types of SCFA, and there were >10 phyla, especially *Acidobacteria*, *Cloacimonetes* and *Hydrogenedentes,* that showed significantly negative association with the accumulation of SCFAs.

Further, a correlation between taxa at genus level and environmental variables was observed (Fig. S5, see online supplementary material). The change of Fe(II) concentration had significantly positive correlations ($P < 0.05$) with genera *Candidatus_Koribacter*, *Candidatus_Solibacter* and *Syntrophorhabdus*, whereas these genera were all significantly negatively correlated ($P < 0.005$) with Fe(III) concentration. In addition, the relative abundances of *Bacillus*, *Clostridium_sensu_stricto_1*, *Clostridium_sensu_stricto_10*, *Clostridium_sensu_stricto_12* and *Desulfitobacterium* were significantly positively correlated ($P < 0.05$) with Fe(III) but negatively correlated with Fe(II). The relative abundance of *Acidovorax*, *Caulobacter* and *Massilia* presented a positive correlation with all six types of SCFA, while the relative abundance of *Candidatus_Solibacter*, *Candidatus_Koribacter*, *Desulfatiglans* and *Syntrophorhabdus* had negative correlation with SCFAs.

DISCUSSION

In the present study, we systematically investigated the variations of biochemical processes including pH, SCFAs as well as Fe(III) reduction and the succession of bacterial community in rice paddy soil caused by the amendment of different types of biochar. Previous studies reported that different biochar feedstocks resulted in the generation of diverse functional groups such as quinone and hydroquinone, which might affect the redox properties of biochar (Zhao *et al.* 2013; Yuan *et al.* 2018). The characterization results in our study also showed that three biochars pyrolysed from different agricultural or forestry wastes (rice straw, orange peel and bamboo powder) under the same pyrolysis conditions harboured similar carbon and oxygen functional groups but differed in their content. In addition, the differences in element content, porosity and pH value of the different types of biochar arose mainly from the original morphology and chemical properties of the feedstocks.

Although there were recoveries of α-diversity during the 90 days of incubation, lower richness of bacterial community and less differential taxa in the three biochar-amended treatments

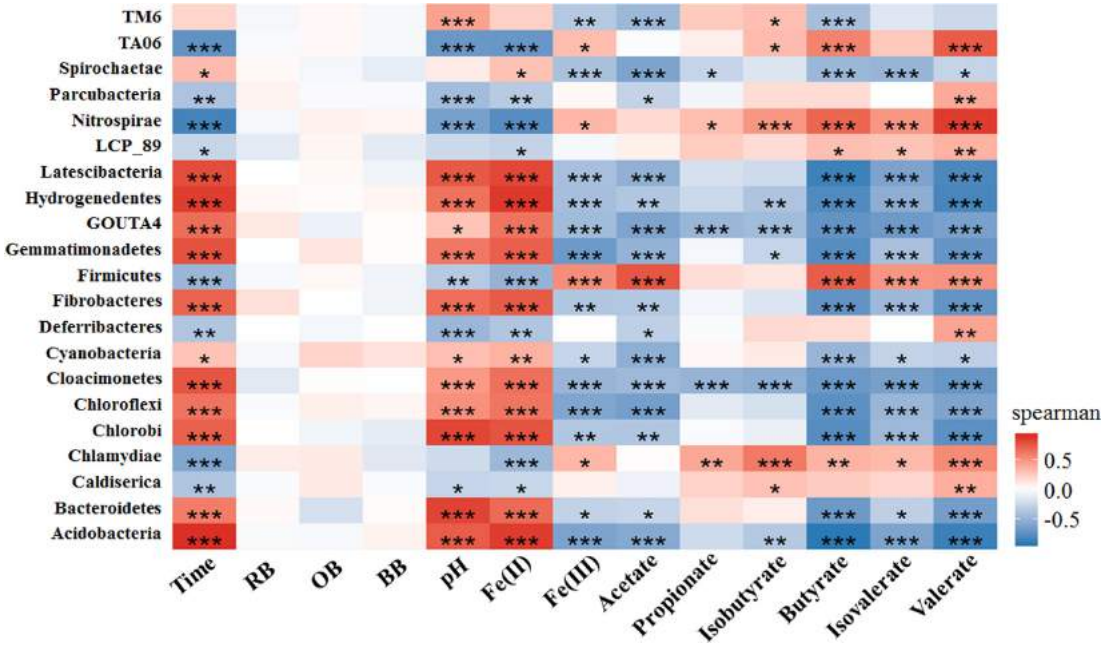

Figure 7. Heatmap of Spearman's correlation coefficient between environmental variables and bacterial taxa at the phylum level. Only taxa that had significant correlations with at least five environmental variables are displayed. *Adjusted *P* value < 0.5; **adjusted *P* value < 0.05; ***adjusted *P* value < 0.005.

in comparison to the NB control were revealed in the α-diversity index and LEfSe results, demonstrating the transitorily negative effect of biochar on bacterial biodiversity. The significant decrease of α-diversity after biochar addition may be caused by the decrease in soil pH, as previous studies found that α-diversity was significantly, positively correlated with pH (Lauber *et al.* 2009; Li *et al.* 2018). Soil pH decreased at day 1 possibly due to the start of anaerobic decomposition of organic matter including acidogenesis (Liu and Zhang 2012), while pH increased after day 1 probably resulting from the dissolution of alkaline functional groups and carbonate (Jia *et al.* 2018). However, the effects were transient and α-diversity recovered afterwards with no significant differences between biochar-amended and NB treatments at day 90, indicating the strong adaptability of the microorganism community; temporal and eventually neutral effects of biochar amendment on bacterial diversity were also reported previously (Cole *et al.* 2019). However, the effect of biochar on microbial diversity was varied and ambiguous due to soil heterogeneity and biochar types. For instance, Feng *et al.* (2012) found that biochar significantly increased proteobacterial abundances, while other studies showed a negative effect of biochar that reduced microbial activity in laboratory incubations (Kurt and Donald 2009). Also in our study, the effect of incubation time on the shift of bacterial community surpassed that caused by different biochar amendment, as NMDS results suggested time was the overriding factor causing the grouping of different samples. Besides, our study showed a drastic succession of bacterial taxa happened in the early stage, and less variance of bacterial community among samples was observed in the late stage of incubation, indicating the high resilience of the soil bacterial community with/without biochar amendment. A 14-month previous study also reported a temporary change of microbial community after biochar addition, in which biochar positively influenced the microbial activity in the first 3 months of incubation, although this effect disappeared in the long-term (Rutigliano *et al.* 2014). The significant successional shift in the microbial community structure over time after biochar addition may due to the character of the biochar as a microbial habitat and labile organic C container (Farrell *et al.* 2013; Quilliam *et al.* 2013). Variation of soil pH with the addition of biochar might also be one reason for the shift of bacterial community as previous studies reported (Bååth and Anderson 2003; Yao *et al.* 2017).

The stimulating effect of biochar on Fe(III) reduction has been reported in much paddy soil research (Jia *et al.* 2018; Wang *et al.* 2017b). Biochar could serve as an electron shuttle between Fe(III)-reducing bacteria and Fe(III) minerals in pure culture (Kappler *et al.* 2014), and further studies revealed that the organic functional groups at the surface of biochar, especially quinones, were responsible for the electron transfer to Fe(III) in paddy soil (Xu *et al.* 2014b). In our study, RB treatment showed slightly higher Fe(III) reduction potential than OB and BB treatments, which might be due to a higher content of C = O in RB. In addition, our study detected that the three biochar-amended treatments all caused higher relative abundance of *Firmicutes* than NB, and LEfSe results showed that all three treatments had significantly abundant taxa that are affiliated to phylum *Proteobacteria* which contains many iron-oxidizing bacteria (Hedrich, Schlomann and Johnson 2011). Therefore the addition of biochar to paddy soil accelerated Fe(III) reduction, which might be due to its stimulating the growth of Fe(III)-reducing bacteria. Furthermore, Spearman's analysis suggested a strong correlation between the relative abundance of typical iron(III)-oxidizing bacteria such as *Bacillus*, *Clostridium* and *Desulfitobacterium* and Fe concentration, and similar relations were also reported previously for a straw biochar applied to soils (Yang *et al.* 2018).

As discussed before, SCFA accumulation showed strong correlation with several bacterial taxa, whose relative abundances were altered by biochar amendment. Many species of *Clostridium* are able to produce organic acids (Abbad-Andaloussi *et al.* 1995; Mitchell 1997; Myszka *et al.* 2012; Dolejš, Rebroš and Rosenberg 2014), and their relative abundance increased in the early stage

for all treatments in our study, correlating with the obvious accumulation of SCFAs. The fast accumulation of SCFAs that resulted from *Clostridia* clusters was also found in the incubation experiment of paddy soil with rice straw (Rui, Peng and Lu 2009). Fast consumption of SCFAs after day 15 was mainly due the growth and activity of SCFA-utilizing bacteria. Butyrate-oxidizing *Syntrophus* and propionate-oxidizing *Syntrophobacter* (Müller *et al.* 2010) were active as they showed negative correlation with SCFA concentration, and other bacterial taxa that negatively associated with SCFA concentration such as *Candidatus_Solibacter*, *Candidatus_Koribacter*, *Defluviicoccus* and *Desulfatiglans* could also take up acetate or propionate (Zhilina *et al.* 2005; Wong and Liu 2007; Müller *et al.* 2010; Suzuki *et al.* 2014). In addition, Fe(III)-reducing bacteria such as *Bacillus* and *Clostridium* that could utilize organic acids as carbon sources and electron donors (Scala *et al.* 2006) also showed negative association with acetate concentration. During anaerobic incubation, Fe(III) reduction and SCFA consumption had a similar pattern, further demonstrating the close relationship between Fe(III) reduction and SCFA consumption previously reported (He and Qu 2008; Li *et al.* 2011).

CONCLUSIONS

Three biochars derived from different feedstocks (rice straw, orange peel and bamboo powder) under the same pyrolysis process showed different micromorphology but similar organic functional groups. The amendment of three different biochars all transiently decreased the biodiversity of soil bacteria but had little influence on bacterial community composition at the end of incubation. Biochar amendment resulted in variation in the SCFA profile and Fe(III) reduction in paddy soil. SCFA-producing as well as Fe(III)-reducing bacteria (e.g. *Clostridia* clusters) were enriched at the early stage, resulting in fast accumulation of SCFAs and Fe(II). Increased SCFA consumption during the incubation was mainly caused by the increased relative abundance of SCFA-utilizing bacteria, such as *Syntrophus*, *Syntrophobacter* and *Desulfatiglans*. To sum up, amendment of different types of biochar led to shifts in the SCFA profile, Fe(III) reduction and bacterial biodiversity in rice paddy soil, however, non-significant differences were observed among the biochars derived from three different agricultural and forestry residues. This finding extends the practical scope of those green wastes and this study expands our knowledge and ability to assess the influence of biochar amendment on the rice cropping ecosystem.

SUPPLEMENTARY DATA

Supplementary data are available at *FEMSEC* online.

FUNDING

This work was supported by the National Natural Science Foundation of China (Grant Nos. 51709100, 51579096, 51521006, and 51222805), the Funds for Innovative Province Construction of Hunan Province of China (2019RS3012), the National Innovative Talent Promotion Program of China (2017RA2088), the Key Research and Development Program of Hunan Province of China (2017SK2241), and the National Program for Support of Top-Notch Young Professionals of China (2012).

Conflict of interest. None declared.

REFERENCES

Abbad-Andaloussi S, Manginot-Durr C, Amine J *et al.* Isolation and characterization of *Clostridium butyricum* DSM 5431 mutants with increased resistance to 1,3-propanediol and altered production of acids. *Appl Environ Microbiol* 1995;**61**:4413–7.

Abdel-Fattah TM, Mahmoud ME, Ahmed SB *et al.* Biochar from woody biomass for removing metal contaminants and carbon sequestration. *J Ind Eng Chem* 2015;**22**:103–9.

Abdelhafez AA, Li J. Removal of Pb(II) from aqueous solution by using biochars derived from sugar cane bagasse and orange peel. *J Taiwan Inst Chem E* 2016;**61**:367–75.

Agegnehu G, Srivastava AK, Bird MI. The role of biochar and biochar-compost in improving soil quality and crop performance: A review. *Appl Soil Ecol* 2017;**119**:156–70.

Awasthi MK, Awasthi SK, Wang Q *et al.* Influence of biochar on volatile fatty acids accumulation and microbial community succession during biosolids composting. *Bioresour Technol* 2018;**251**:158–64.

Bååth E, Anderson TH. Comparison of soil fungal/bacterial ratios in a pH gradient using physiological and PLFA-based techniques. *Soil Biol Biochem* 2003;**35**:955–63.

Bolger AM, Lohse M, Usadel B. Trimmomatic: a flexible trimmer for Illumina sequence data. *Bioinformatics* 2014;**30**:2114–20.

Caporaso JG, Kuczynski J, Stombaugh J *et al.* QIIME allows analysis of high-throughput community sequencing data. *Nat Methods* 2010;**7**:335–6.

Cayuela ML, Van Zwieten L, Singh BP *et al.* Biochar's role in mitigating soil nitrous oxide emissions: A review and meta-analysis. *Agr Ecosyst Environ* 2014;**191**:5–16.

Chen X. Economic potential of biomass supply from crop residues in China. *Appl Energ* 2016;**166**:141–9.

Cole EJ, Zandvakili OR, Blanchard J *et al.* Investigating responses of soil bacterial community composition to hardwood biochar amendment using high-throughput PCR sequencing. *Appl Soil Ecol* 2019;**136**:80–5.

Dolejš I, Rebroš M, Rosenberg MJ. Immobilisation of *Clostridium* spp. for production of solvents and organic acids. *Chem Pap* 2014;**68**:1–14.

Edgar RC, Haas BJ, Clemente JC *et al.* UCHIME improves sensitivity and speed of chimera detection. *Bioinformatics* 2011;**27**:2194–200.

Farrell M, Kuhn TK, Macdonald LM *et al.* Microbial utilisation of biochar-derived carbon. *Sci Total Environ* 2013;**465**:288–97.

Feng Y, Xu Y, Yu Y *et al.* Mechanisms of biochar decreasing methane emission from Chinese paddy soils. *Soil Biol Biochem* 2012;**46**:80–8.

Foggo A, Rundle SD, Bilton DT. The net result: evaluating species richness extrapolation techniques for littoral pond invertebrates. *Freshwater Biol* 2003;**48**:1756–64.

Gul S, Whalen JK. Biochemical cycling of nitrogen and phosphorus in biochar-amended soils. *Soil Biol Biochem* 2016;**103**:1–15.

He J, Qu D. Dissimilatory Fe(III) reduction characteristics of paddy soil extract cultures treated with glucose or fatty acids. *J Environ Sci* 2008;**20**:1103–8.

Hedrich S, Schlomann M, Johnson DB. The iron-oxidizing proteobacteria. *Microbiology* 2011;**157**:1551–64.

Hussain M, Farooq M, Nawaz A *et al.* Biochar for crop production: potential benefits and risks. *J Soil Sediment* 2016;**17**:685–716.

Jia R, Li L, Qu D *et al.* Enhanced iron(III) reduction following amendment of paddy soils with biochar and glucose modified biochar. *Environ Sci Pollut R* 2018;**25**:91–103.

Kappler A, Wuestner ML, Ruecker A *et al*. Biochar as an electron shuttle between bacteria and Fe(III) minerals. *Environ Sci Tech Let* 2014;**1**:339–44.

Kloss S, Zehetner F, Dellantonio A *et al*. Characterization of slow pyrolysis biochars: effects of feedstocks and pyrolysis temperature on biochar properties. *J Environ Qual* 2012;**41**:990–1000.

Kurt AS, Donald CR. Impacts of sixteen different biochars on soil greenhouse gas production. *Ann Environ Sci* 2009;**3**:179–93.

Lauber CL, Hamady M, Knight R *et al*. Pyrosequencing-based assessment of soil pH as a predictor of soil bacterial community structure at the continental scale. *Appl Environ Microbiol* 2009;**75**:5111–20.

Li H, Peng J, Weber KA *et al*. Phylogenetic diversity of Fe(III)-reducing microorganisms in rice paddy soil: enrichment cultures with different short-chain fatty acids as electron donors. *J Soil Sediment* 2011;**11**:1234–42.

Li Q, Lei Z, Song X *et al*. Biochar amendment decreases soil microbial biomass and increases bacterial diversity in Moso bamboo (*Phyllostachys edulis*) plantations under simulated nitrogen deposition. *Environ Res Lett* 2018;**13**:044029.

Li X, Zhang W, Liu T *et al*. Changes in the composition and diversity of microbial communities during anaerobic nitrate reduction and Fe(II) oxidation at circumneutral pH in paddy soil. *Soil Biol Biochem* 2016;**94**:70–9.

Liu XH, Zhang XC. Effect of biochar on pH of alkaline soils in the Loess Plateau: results from incubation experiments. *Int J Agric Biol* 2012;**14**:65–70.

Liu Y, Lu H, Yang S *et al*. Impacts of biochar addition on rice yield and soil properties in a cold waterlogged paddy for two crop seasons. *Field crop res* 2016;**191**:161–7.

Lu K, Yang X, Gielen G *et al*. Effect of bamboo and rice straw biochars on the mobility and redistribution of heavy metals (Cd, Cu, Pb and Zn) in contaminated soil. *J Environ Manage* 2017;**186**:285–92.

Lu W, Ding W, Zhang J *et al*. Biochar suppressed the decomposition of organic carbon in a cultivated sandy loam soil: A negative priming effect. *Soil Biol Biochem* 2014;**76**:12–21.

Lu Y, Fu L, Lu Y *et al*. Effect of temperature on the structure and activity of a methanogenic archaeal community during rice straw decomposition. *Soil Biol Biochem* 2015;**81**:17–27.

Ma K, Conrad R, Lu Y. Responses of methanogen *mcrA* genes and their transcripts to an alternate dry/wet cycle of paddy field soil. *Appl Environ Microbiol* 2012;**78**:445–54.

Mitchell WJ. Physiology of carbohydrate to solvent conversion by clostridia. *Adv Microb Physiol* 1997;**39**:31–130.

Müller N, Worm P, Schink B *et al*. Syntrophic butyrate and propionate oxidation processes: from genomes to reaction mechanisms. *J Environ Manage* 2010;**2**:489–99.

Myszka K, Leja K, Olejnik-Schmidt AK *et al*. Isolation process of industrially useful *Clostridium bifermentans* from natural samples. *J Biosci Bioeng* 2012;**113**:631–3.

Oksanen J, Kindt R, Legendre P *et al*. Vegan: community ecology package. R package version 1.13-1.: http://vegan.r-forge.r-project.org/. 2008 .

Qambrani NA, Rahman MM, Won S *et al*. Biochar properties and eco-friendly applications for climate change mitigation, waste management, and wastewater treatment: A review. *Renew Sust Energ Rev* 2017;**79**:255–73.

Qiao JT, Li XM, Li FB. Roles of different active metal-reducing bacteria in arsenic release from arsenic-contaminated paddy soil amended with biochar. *J Hazard Mater* 2018;**344**:958–67.

Quilliam RS, Glanville HC, Wade SC *et al*. Life in the 'charosphere' - Does biochar in agricultural soil provide a significant habitat for microorganisms? *Soil Biol Biochem* 2013;**65**:287–93.

Ramos A, Monteiro E, Silva V *et al*. Co-gasification and recent developments on waste-to-energy conversion: A review. *Renew Sust Energ Rev* 2018;**81**:380–98.

Reyon D, Tsai SQ, Khayter C *et al*. FLASH assembly of TALENs for high-throughput genome editing. *Nat Biotechnol* 2012;**30**:460–5.

Rui J, Peng J, Lu Y. Succession of bacterial populations during plant residue decomposition in rice field soil. *Appl Environ Microbiol* 2009;**75**:4879–86.

Rutigliano FA, Romano M, Marzaioli R *et al*. Effect of biochar addition on soil microbial community in a wheat crop. *Eur J Soil Biol* 2014;**60**:9–15.

Scala DJ, Hacherl EL, Cowan R *et al*. Characterization of Fe(III)-reducing enrichment cultures and isolation of Fe(III)-reducing bacteria from the Savannah River site, South Carolina. *Res Microbiol* 2006;**157**:772–83.

Song Y, Bian Y, Wang F *et al*. Effects of biochar on dechlorination of hexachlorobenzene and the bacterial community in paddy soil. *Chemosphere* 2017;**186**:116–23.

Suzuki D, Li Z, Cui X *et al*. Reclassification of *Desulfobacterium anilini* as *Desulfatiglans anilini* comb. nov. within *Desulfatiglans* gen. nov., and description of a 4-chlorophenol-degrading sulfate-reducing bacterium, *Desulfatiglans parachlorophenolica* sp. nov. *Inter J Syst Evol Micr* 2014;**64**:3081–6.

Tang L, Yu J, Pang Y *et al*. Sustainable efficient adsorbent: Alkali-acid modified magnetic biochar derived from sewage sludge for aqueous organic contaminant removal. *Chem Eng J* 2018;**336**:160–9.

ter Braak CJ, Smilauer P. *Canoco Reference Manual and User's Guide: Software for Ordination, Version* 5.0. NY, USA: Microcomputer Power, 2012.

Tian J, Wang J, Dippold M *et al*. Biochar affects soil organic matter cycling and microbial functions but does not alter microbial community structure in a paddy soil. *Sci Total Environ* 2016;**556**:89–97.

Tong H, Hu M, Li FB *et al*. Biochar enhances the microbial and chemical transformation of pentachlorophenol in paddy soil. *Soil Biol Biochem* 2014;**70**:142–50.

Wang C, Shen J, Liu J *et al*. Microbial mechanisms in the reduction of CH_4 emission from double rice cropping system amended by biochar: A four-year study. *Soil Biol Biochem* 2019b;**135**:251–63.

Wang G, Li Q, Gao X *et al*. Synergetic promotion of syntrophic methane production from anaerobic digestion of complex organic wastes by biochar: Performance and associated mechanisms. *Bioresour Technol* 2018;**250**:812–20.

Wang M, Ren L, Wang D *et al*. Assessing the capacity of biochar to stabilize copper and lead in contaminated sediments using chemical and extraction methods. *J Environ Sci* 2019a;**79**:91–9.

Wang N, Xue XM, Juhasz AL *et al*. Biochar increases arsenic release from an anaerobic paddy soil due to enhanced microbial reduction of iron and arsenic. *Environ Pollut* 2017b;**220**:514–22.

Wang P, Tang L, Wei X *et al*. Synthesis and application of iron and zinc doped biochar for removal of p-nitrophenol in wastewater and assessment of the influence of co-existed Pb(II). *Appl Surf Sci* 2017a;**392**:391–401.

Wang Q, Garrity GM, Tiedje JM *et al*. Naive Bayesian classifier for rapid assignment of rRNA sequences into the new bacterial taxonomy. *Appl Environ Microbiol* 2007;**73**:5261–7.

Wong MT, Liu WT. Ecophysiology of *Defluviicoccus*-related tetrad-forming organisms in an anaerobic-aerobic activated sludge process. *Environ Microbiol* 2007;**9**:1485–96.

Xiao X, Chen B, Zhu L. Transformation, morphology, and dissolution of silicon and carbon in rice straw-derived biochars under different pyrolytic temperatures. *Environ Sci Technol* 2014;**48**:3411–9.

Xie H, Zhang D, Mao G *et al*. Availability of lignocellulose from forestry waste for use as a biofuel in China. *3 Biotech* 2018;**8**:234.

Xu HJ, Wang XH, Li H *et al*. Biochar impacts soil microbial community composition and nitrogen cycling in an acidic soil planted with rape. *Environ Sci Technol* 2014a;**48**:9391–9.

Xu Y, Lou Z, Yi P *et al*. Improving abiotic reducing ability of hydrothermal biochar by low temperature oxidation under air. *Bioresour Technol* 2014b;**172**:212–8.

Yang YP, Zhang HM, Yuan HY *et al*. Microbe mediated arsenic release from iron minerals and arsenic methylation in rhizosphere controls arsenic fate in soil-rice system after straw incorporation. *Environ Pollut* 2018;**236**:598–608.

Yao Q, Liu J, Yu Z *et al*. Changes of bacterial community compositions after three years of biochar application in a black soil of northeast China. *Appl Soil Ecol* 2017;**113**:11–21.

Yoon J, Ishikawa S, Kasai H *et al*. *Perexilibacter aurantiacus* gen. nov., sp. nov., a novel member of the family '*Flammeovirgaceae*' isolated from sediment. *Inter J Syst Evol Micr* 2007;**57**:964–8.

Yuan H, Chen Y, Zhang H *et al*. Improved bioproduction of short-chain fatty acids (SCFAs) from excess sludge under alkaline conditions. *Environ Sci Technol* 2006;**40**:2025–9.

Yuan HY, Ding LJ, Zama EF *et al*. Biochar modulates methanogenesis through electron syntrophy of microorganisms with ethanol as a substrate. *Environ Sci Technol* 2018;**52**:12198–207.

Zhao L, Cao X, Masek O *et al*. Heterogeneity of biochar properties as a function of feedstock sources and production temperatures. *J Hazard Mater* 2013;**256-257**:1–9.

Zhilina T, Zavarzina D, Kolganova T *et al*. "*Candidatus* Contubernalis alkalaceticum," an obligately syntrophic alkaliphilic bacterium capable of anaerobic acetate oxidation in a coculture with *Desulfonatronum cooperativum*. *Microbiology* 2005;**74**:695–703.

Zuur A, Ieno EN, Meesters E. *A Beginner's Guide to R*. Springer Science & Business Media, 2009.